Supporting Information

Seasonal risk assessment of water-electricity nexus systems under water consumption policy constraint

Mengfei Mu[1,2,3], Zhenxing Zhang[3*], Ximing Cai[4], Qiuhong Tang[1,2*]

[1] Key Laboratory of Water Cycle and Related Land Surface Processes, Institute of Geographical Sciences and Natural Resources Research, Chinese Academy of Sciences, Beijing, China

[2] University of Chinese Academy of Sciences, Beijing, China

[3] Illinois State Water Survey, Prairie Research Institute, University of Illinois at Urbana-Champaign, Champaign, IL, United States

[4] Department of Civil and Environmental Engineering, University of Illinois at Urbana-Champaign, Urbana, IL, United States

Corresponding authors:

Zhenxing Zhang (zhang538@illinois.edu)

Qiuhong Tang (tangqh@igsnrr.ac.cn)

10 Pages, 4 Figures and 1 Table included

S-1 Input data sources

Climate data used in this study include daily air temperature, air pressure, and specific humidity obtained from the North American Land Data Assimilation System project phase 2 (NLDAS-2) dataset[1,2]. The temporal resolution of the NLDAS-2 dataset is hourly and is rescaled to a daily average basis to match the temporal resolution of this study. The spatial resolution of the NLDAS-2 is 0.125 degrees (around 12 km). The grid where the power plant is located and the eight surrounding grids are selected. The data in those nine grids are averaged to reduce the uncertainty and represent the daily climate conditions at the power plant.

Data on basic plant characteristics, such as the geographic location, maximum capacity, fuel type, and cooling system type, are obtained from the Energy Information Administration Form 860 (EIA-860) database[3] to set up the Integrated Environmental Control Model (IECM)[4–6].

The site-specific daily streamflow data from 1982-2012 are obtained from the U.S. Geological Survey National Water Information System (NWIS)[7] to represent local water resources condition.

S-2 Study areas

A comparative assessment is conducted in two representative watersheds in the United states to reveal the differences in seasonal risk of the water-electricity nexus under the same environmental policy constraint. The Kaskaskia River watershed (Figure S1a) in southern Illinois in the US Midwest is selected as a relatively wet watershed. The observed long-term average streamflow in this watershed is $113\ m^3/s$ at the gage station shown in Figure S1a. The San Juan River watershed located near the Four Corners region of Colorado, Utah, Arizona, and New

Mexico in the US Southwest is selected as a relatively dry watershed. The observed long-term average streamflow at this watershed is $52\ \mathrm{m}^3/s$, which is only about 46% of that in the Kaskaskia River watershed. The two power plants, i.e., the Prairie State Generating Station (Plant A) in the Kaskaskia River watershed and the San Juan Generating Station (Plant B) in the San Juan River watershed, are selected as they have similar plant characteristics (See Table S1). For example, they share the same fuel type (coal-fired), the same cooling technology (wet cooling tower), a similar maximum capacity ($1628\ MW$ and $1648\ MW$), and a similar long-term average electricity generation output ($1154\ MW$ and $1164\ MW$). However, the climate and streamflow conditions in these two watersheds are very different and would lead to different cooling water intensities, availability, and consumption as well as their temporal distributions. A comparative assessment in these two watersheds is described in the Results Section.

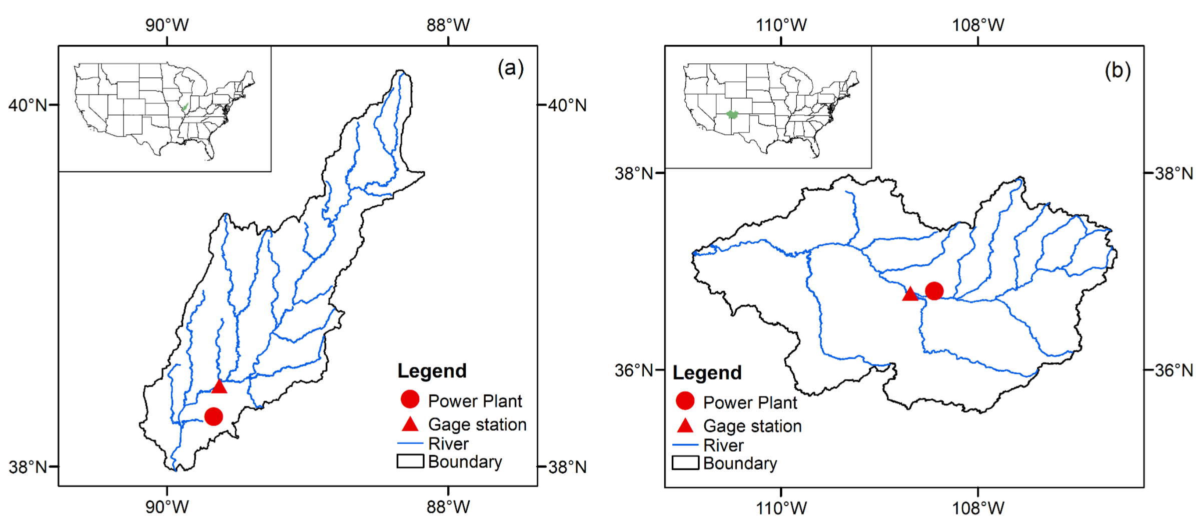

Figure S1. (a) Kaskaskia River watershed in Illinois state of the US Midwest and (b) San Juan River watershed in the US Southwest.

Table S1. The two power plants in two representative watersheds and their characteristics

	Plant A	Plant B
Located Watershed	Kaskaskia	San Juan
Average Air Temperature (℃)	14	14
Average Relative Humidity (%)	74	42
Average Streamflow (m^3/s)	113	52
Fuel	Coal	Coal
Cooling System	Wet Cooling Tower	Wet Cooling Tower
Maximum Capacity (MW)	1628	1848
Average output (MW)	1154	1164
Average Cooling Water Intensity (m^3/MWh)	1.83	1.98

S-3 The fundamentals of cooling water consumption estimation module in IECM

Based on the water mass balance of the wet cooling tower, the cooling water consumption (WC) is the makeup water which is fed to the boiler to maintain the cooling process[4,5]. The cooling water consumption rate equals to the makeup water rate (m) and can be estimated as:

$$m = \frac{\beta}{1-\beta} m_s + \eta_s * m_s \qquad (S1)$$

where β is the boiler blowdown rate (% of the feedwater), η_s is the miscellaneous loss (%), m_s is the steam flow rate $(10^3\ kg/hr)$ in the boiler. m_s depends on the steam cycle heat rate, gross power output, and boiler characteristic, and can be estimated as:

$$m_s = \frac{Hr_s * MW_g}{\left(h_s^{super} - h_w^{boiler}\right) + \phi_{reheat} * \left(h_{s,out}^{reheat} - h_{s,in}^{reheat}\right)} \qquad (S2)$$

where Hr_s is the steam cycle heat rate (kJ/kWh), MW_g is the gross power output (MW), h_s^{super} is the boiler superheat steam enthalpy (kJ/kg), h_w^{boiler} is the boiler feedwater enthalpy (kJ/kg),

ϕ_{reheat} is the mass fraction of reheat steam, $h_{s,out}^{reheat}$ is the steam enthalpy after the reheat (kJ/kg), $h_{s,in}^{reheat}$ is the steam enthalpy before the reheat (kJ/kg). For more detailed explanation and calculation, please refer to IECM documentation[4–6].

S-4 Sensitivity test of cooling water consumption intensity to air temperature and relative humidity

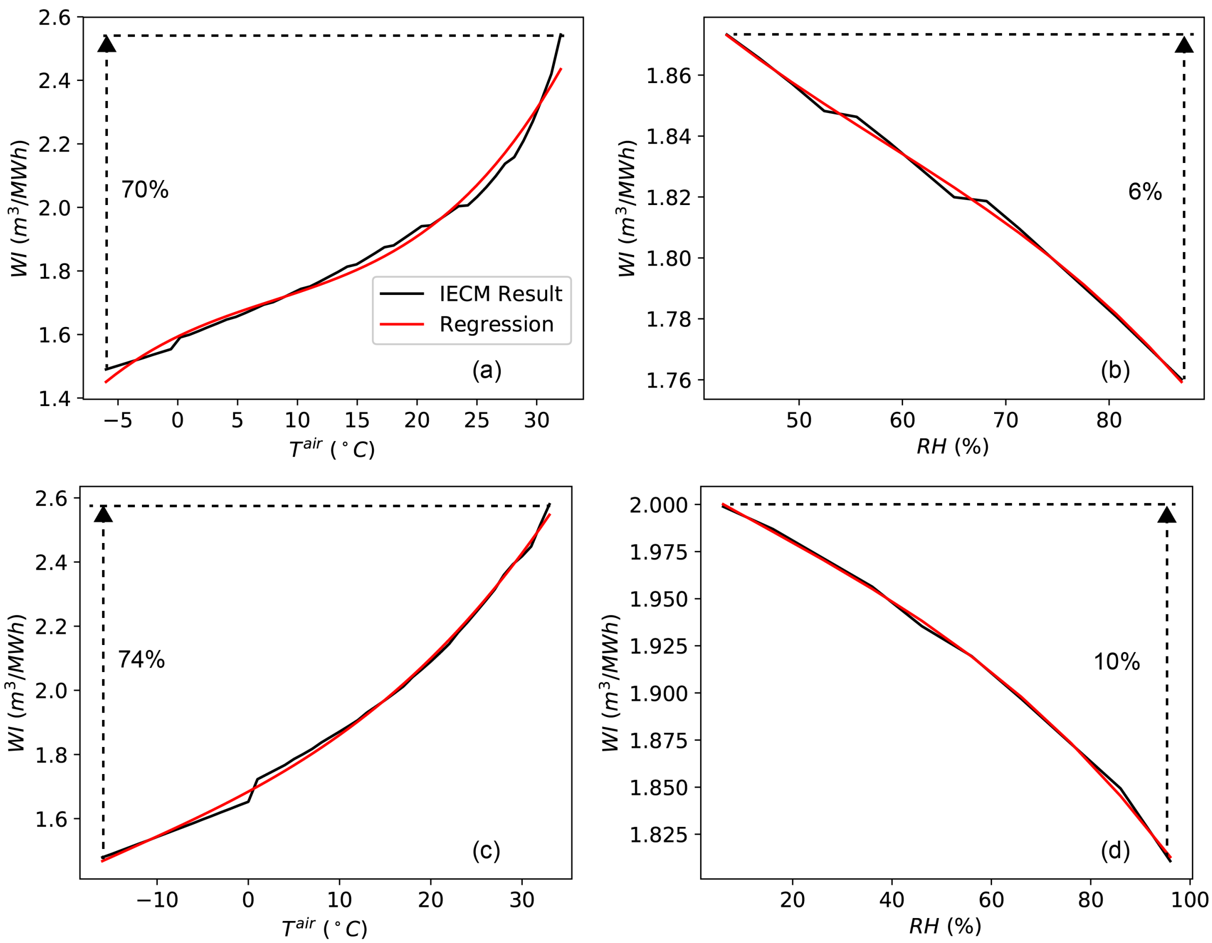

Figure S2. Sensitivities of cooling water consumption intensity (WI) to (a) and (c) air temperature (T^{air}) and (b) and (d) relative humidity (RH) at a coal-fired power plant with a wet cooling tower in the Kaskaskia River watershed and San Juan River watershed, respectively.

S-5 Seasonality of cooling water consumption intensity

This section demonstrates the significant seasonality of the WI and the necessity of using variable WIs to consider the impacts of variations in climate conditions rather than using an average WI as in previous studies to estimate the cooling water consumption. Figure 2 shows the daily WI during 1982-2012, the mean daily WI, and the long-term average of the daily WI at the two coal-fired power plants in the two watersheds. At the plant in the Kaskaskia (San Juan) River watershed in Figure 2a (2b), the daily WI (red line) would be underestimated by as much as 50% (28%) during summer seasons and overestimated by 80% (26%) during the winter seasons if using a constant long-term average value (black dashed line). In the long run during 1982-2012, the mean daily WI (black solid line) would be underestimated in the summer by 20% (20%) and overestimated in the winter by 18% (16%), as in Figure 2a (2b). The average of the WI in the Kaskaskia watershed (Figure 2a) is a bit smaller than that in the San Juan (Figure 2b) but with a larger variability, e.g., a very large WI during summer and a small WI during winter in some years caused by extremely high or low temperatures in the Kaskaskia watershed. The seasonal variability of the WI is found to be significant compared to the interannual changes $(6{\sim}10\%)$ of the WI in the context of climate change (RCP 8.5 scenario)[8]. Overlooking the temporal variability of the WI would lead to underestimates of the water-electricity nexus risk in dry seasons, especially in drought events. Therefore, it is necessary to use the variable WIs to estimate cooling water consumption and the associated seasonal risk of the water-electricity nexus.

S-6 Constrained usable capacity under water consumption policy constraint

The section demonstrates the constrained usable capacity under some specific water consumption policy constraint during a representative undersupply period in Kaskaskia and San Juan River watershed. A strict and a relaxed policy constraint are chosen in each watershed.

In Kaskaskia (Figure S3a), when a strict policy constraint, i.e., a small R^0, is adopted, the usable capacity shown by the red solid line is far below the historic power output shown by the black solid line from May to November of the year 1988, which is an extreme drought period in this watershed. When R^0 is increased to 25%, which means more water is accessible by the power plant each day to support power generation, the usable capacity in most days (and all days in the typical dry ASO season) are increased beyond the historic power output. The usable capacity reaches to the maximum capacity and appears as a flat line in some days, e.g., in May. However, some extremely dry days, i.e., in June, would still suffer from the electricity undersupply even under such a relaxed policy constraint. This explains why the $MaxT$ value of MJJ season is larger than that of ASO season in Figure 5 when R^0 is larger than 20%. In San Juan (Figure S3b), the longest period of the potential electricity undersupply lasts from March to September of the year 2002, with the most serious risk occurring in July. Compared to Kaskaskia, a smaller R^0 can increase usable capacity in San Juan to a high level, which is also verified in Figure 5b and 5d.

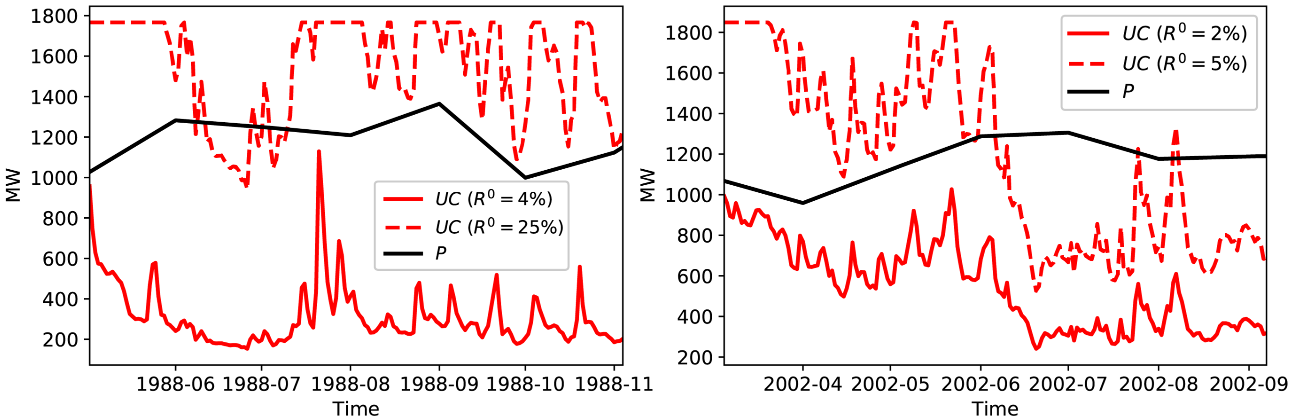

(a) Kaskaskia River watershed (b) San Juan River watershed

Figure S3. Constrained usable capacity under a strict (red solid line) and relaxed (red dashed line) water consumption policy constraint and historic power output (black solid line) during the representative potential risky period at the power plant in (a) Kaskaskia River watershed and (b) San Juan River watershed.

S-7 Constrained cooling water consumption under water consumption policy constraint

Under a specific cooling water consumption policy constraint, the power plants may be constrained with less water availability and power generation, while water resources can be conserved for other water users. This section demonstrates the constrained cooling water consumption during a representative undersupply period in Kaskaskia and San Juan River watershed under the same policy constraints as in Section S-6.

In Figure S4, when a strict policy constraint, i.e., a small R^0, is adopted, the water consumption shown by the red solid line in both watersheds is far below the historic water consumption rate. In this case, a large amount of water can be conserved and transferred to other water users, while power generation would be reduced as shown in Figure S3. When R^0 is increased to a higher level, i.e., 25% in Kaskaskia and 5% in San Juan, water consumption in most days would approach the historic level to support power generation, especially in Kaskaskia River watershed.

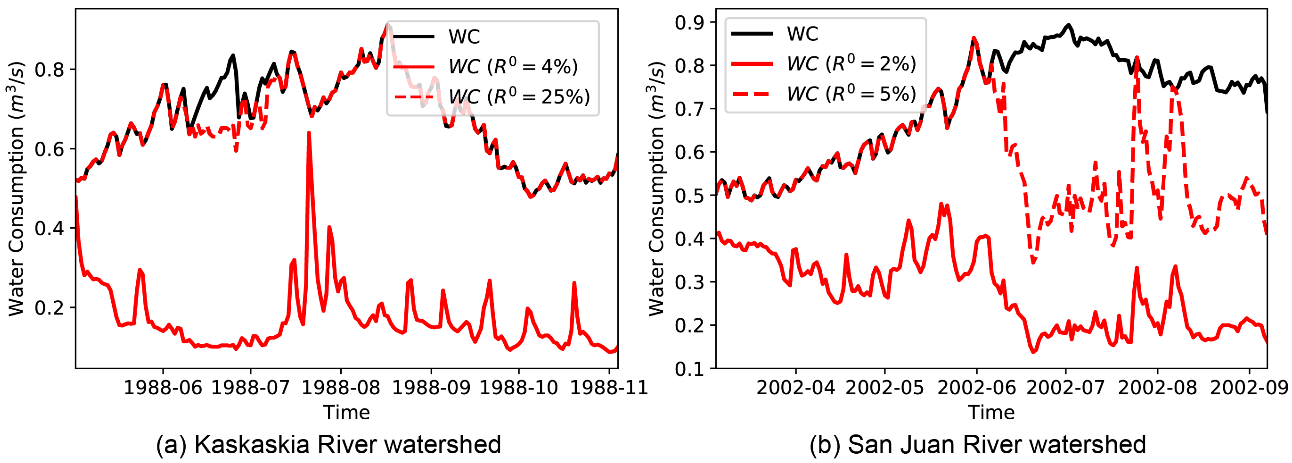

Figure S4. Cooling water consumption under a strict (red solid line) and relaxed (red dashed line) water consumption policy constraint and historic cooling water consumption (black solid line) at the power plant in (a) Kaskaskia River watershed and (b) San Juan River watershed.

References

(1) Xia, Y.; Mitchell, K.; Ek, M.; Cosgrove, B.; Sheffield, J.; Luo, L.; Alonge, C.; Wei, H.; Meng, J.; Livneh, B.; Duan, Q., Lohmann, D. Continental-Scale Water and Energy Flux Analysis and Validation for North American Land Data Assimilation System Project Phase 2 (NLDAS-2): 2. Validation of Model-Simulated Streamflow. *J. Geophys. Res. Atmospheres* **2012**, *117* (D3). https://doi.org/10.1029/2011JD016051.

(2) Xia, Y.; Mitchell, K.; Ek, M.; Sheffield, J.; Cosgrove, B.; Wood, E.; Luo, L.; Alonge, C.; Wei, H.; Meng, J.; Livneh, B., Lettenmaier, D., Koren, V., Duan, Q., Mo, K., Fan, Y., Mocko, D. Continental-Scale Water and Energy Flux Analysis and Validation for the North American Land Data Assimilation System Project Phase 2 (NLDAS-2): 1. Intercomparison and Application of Model Products. *J. Geophys. Res. Atmospheres* **2012**, *117* (D3). https://doi.org/10.1029/2011JD016048.

(3) EIA. Form EIA-860 Detailed Data https://www.eia.gov/electricity/data/eia860/ (accessed Apr 18, 2018).

(4) Berkenpas, M. P.; Kietzke, K.; Mantripragada, H.; McCoy, S. T.; Rubin, E. S.; Versteeg, P. L.; Zhai, H. IECM Technical Documentation Updates Final Report. **2009**, *1–5*.
(5) Zhai, H.; Rubin, E. S.; Versteeg, P. L. Water Use at Pulverized Coal Power Plants with Postcombustion Carbon Capture and Storage. *Environ. Sci. Technol.* **2011**, *45* (6), 2479–2485. https://doi.org/10.1021/es1034443.
(6) Berkenpas, M. B.; Fry, J. J.; Kietzke, K.; Rubin, E. S. IECM User Documentation: User Manual. 2018.
(7) USGS. National Water Information System http://waterdata.usgs.gov/nwis (accessed Apr 1, 2018).
(8) Talati, S.; Zhai, H.; Kyle, G. P.; Morgan, M. G.; Patel, P.; Liu, L. Consumptive Water Use from Electricity Generation in the Southwest under Alternative Climate, Technology, and Policy Futures. *Environ. Sci. Technol.* **2016**, *50* (22), 12095–12104. https://doi.org/10.1021/acs.est.6b01389.